Adsorption of Aqueous Nucleobases, Nucleosides, and Nucleotides on Humic Acids. 3. Adsorption of Uracil, Uridine, and Uridine-5′-Monophosphate on a German Peat-Derived Humic Acid and Its Tightly Bound Mercury(II) Form

Elham A. Ghabbour,*,† Geoffrey Davies,*,‡ Amjad Fataftah,‡ Nadeem K. Ghali,‡,§ Melissa E. Goodwillie,‡,§ Susan A. Jansen,|| and Nichole A. Smith‡,§

Soil Salinity Laboratory, Agricultural Research Center, Bacos, Alexandria 21616, Egypt, Chemistry Department and the Barnett Institute, Northeastern University, Boston, Massachusetts 02115, and Chemistry Department, Temple University, Philadelphia, Pennsylvania 19122

Received: February 24, 1997; In Final Form: June 17, 1997[⊗]

Aqueous nucleic acid constituents uracil, uridine, and uridine-5′-monophosphate are selectively adsorbed by a solid German peat-derived humic acid (GHA) and its tightly bound mercury(II) form (MGHA). Adsorption isotherms with GHA and MGHA adsorbents were obtained at 19 solute concentrations from 0 to 1.20 mM and seven fixed temperatures from 5.0 to 35.0 °C. Langmuir data analysis indicates that adsorption occurs in sequential steps A, B, and C, depending on the solute and experimental conditions. MGHA very strongly adsorbs low concentrations of uracil and site capacity v_A for uracil adsorption on MGHA in step A increases with increasing temperature. The last steps of adsorption of relatively high concentrations of uridine, and uridine-5′-monophosphate on MGHA are S-curves ascribed to increasing site capacity with increasing solute concentration. Comparison of the new data for adsorbents GHA and MGHA with data for adsorption of uracil, uridine, and uridine-5′-monophosphate on compost-derived humic acid (CHA) from part 1 reveals similarities and differences. Nevertheless, linear plots of adsorption enthalpies vs entropies in all detected steps with CHA, GHA, and MGHA as adsorbents indicate that selective adsorption of nucleic acid constituents on different HAs is free energy buffered by similar mechanisms.

Introduction

Humic acids (HAs) are highly functionalized organic macromolecules in animals,[1] plants,[2,3] soils,[4] and sediments.[5] HAs are versatile materials with many environmental roles. They stabilize soils and sediments and regulate the levels of water, metals, and other components.[4−8] HAs in soils[2,4,6,8] and plants[2,3] are attached to clays and minerals, and they bind metals, polysaccharides, and proteins.[4,6,9] The properties of HA samples thus depend on their source, how they are isolated as aqueous gels, and how the dried materials are handled.[1−8] We isolate HAs with methods[2,10,11] that minimize contaminants, maximize HA yields, and hopefully preserve HA molecular structures.

Most herbicides and pesticides are *sorbed* by humic substances by partition between water and "organic liquidlike" hydrophobic regions as well as *adsorbed* more selectively by stacked structural features and HA functional groups.[12] Naturally occurring nucleic acid constituents (NACs) are polar, hydrophilic solutes. NACs are useful for adsorption studies because they exist as structurally related triads such as uracil, uridine, and uridine-5′-monophosphate, which all have a uracil nucleobase unit.

Parts 1[13] and 2[14] show that selective adsorption of NACs on compost-derived humic acid CHA occurs in sequential steps A, B, and C with increasing solute concentration. Analysis of the isotherm segments with the Langmuir model for reversible adsorption gives a site capacity v_i and equilbrium constant K_i for each solute and adsorption step *i*. We concluded from v_i comparisons that NACs adsorb through their nucleobase units. Studies at different temperatures revealed that adsorption can be endothermic, thermoneutral, or exothermic, depending on the solute and adsorption step. Linear correlation of adsorption enthalpies ΔH_i and entropies ΔS_i for all solutes in all adsorption steps *i* indicated that CHA behaves as a free energy buffer in its interactions with NACs.[15]

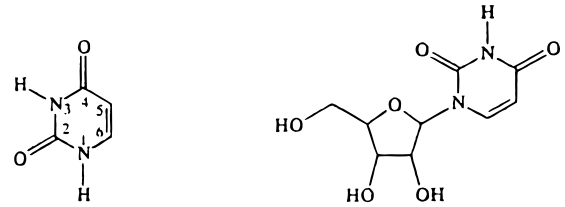

uracil

uridine

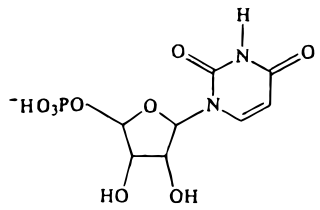

uridine-5'-monophosphate

This paper reports data for adsorption of uracil, uridine, and uridine-5′-monophosphate on a humic acid isolated from German peat (GHA) and its tightly bound mercury(II) form (MGHA). The solutes were chosen because they all have the uracil nucleobase unit and CHA has unusually low capacity for uridine.[13] This solute choice is important because other NACs

† Soil Salinity Laboratory.
‡ Northeastern University.
§ Undergraduate research student.
|| Temple University.
⊗ Abstract published in *Advance ACS Abstracts,* September 1, 1997.

S1089-5647(97)00665-2 CCC: $14.00

such as adenine have the ability to free up ("create") more sites after primary adsorption.[15] Mercury(II) was chosen to investigate the effect of a metal on HAs adsorption characteristics because (a) mercury is toxic; (b) Hg(II) often exhibits 2-coordination in its complexes[16] whereas most other metals prefer higher coordination numbers; and (c) most metals bind nucleotides through their nucleobases and phosphate groups whereas "soft" Hg(II) prefers the "soft," pseudoaromatic nucleobase of uridine and uridine-5′-monophosphate.[17−20] The present results are compared with previous[13] data for NAC adsorption on CHA to address these questions.

(1) Do HAs from different sources selectively adsorb NAC solutes and can the isotherm segments be analyzed with the Langmuir model?

(2) How do the v_i and thermodynamic parameters K_i, ΔH_i and ΔS_i for sequential solute adsorption on HAs from different sources compare?

(3) What are the effects of a tightly bound metal such as mercury(II) on the adsorption parameters?

(4) Are the enthalpies ΔH_i and entropies ΔS_i for adsorption on HAs and metal-loaded HAs from different sources correlated?

Experimental Section

Materials. Uracil, uridine, uridine-5′-monophosphate, and mercury(II) acetate were used as supplied by Sigma. Doubly deionized water was employed throughout. The humic acid adsorbent GHA of this study was isolated from German peat provided by Staatsbad Pyrmont AG, Bad Pyrmont, Germany.

The peat sample was sieved to remove twigs and rocks and then dried overnight under vacuum at 40 °C. The ground, dried sample was Soxhlet extracted with 2:1 v/v benzene/methanol to remove nonhumic substances.[10] Extraction was continued until the extracting solvent had negligible absorbance. The residue was washed by shaking five times with 0.1 M HCl to remove metals and minerals[21] and five times with water. All these and succeeding washings were conducted with centrifugation at room temperature. The residue then was shaken at room temperature in a filled, tightly closed container with 0.1 M NaOH overnight and centrifuged. The supernatant was brought to pH 1.0 by addition of concentrated HCl, and the aqueous gel that settled overnight was isolated by centrifugation. Residue extraction with NaOH and gel formation from the supernatants with HCl were continued until no more gel was obtained at pH 1.0. The gels from all the extraction cycles were combined and washed five times with a HF/HCl solution[22] to remove metals and minerals and five times with water. The resulting gel was chilled to 77 K and freeze dried in a Labconco lyophilizer to give brown solid GHA. The GHA yield was 27% w/w on a dry source weight basis.

Tightly bound mercury(II) sample MGHA was obtained by shaking solid GHA (1.50 g) with 1.5 L of aqueous 0.1 M mercury(II) acetate for 48 h at room temperature. The loaded solid was separated by centrifugation and washed five times by shaking with water and centrifugation to remove excess and weakly bound Hg. The washed solid was freeze dried to give brown solid MGHA.

Dry solids GHA and MGHA were homogenized by vigorous mechanical shaking for 48 h and stored at room temperature in tightly closed containers.

Analyses. Elemental C, H, N analysis of GHA was conducted by Galbraith Laboratories, Knoxville, TN. Mercury in MGHA was analyzed as follows. A weighed amount of MGHA was digested with boiling 1:1 v/v $HNO_3/HClO_4$. After cooling to room temperature, 1 mL of 48% w/v HF was added to dissolve silicates. Each analyte solution was made up to the mark with 0.1 M H_3BO_3 (to suppress spectrometric fluorine interference) in a calibrated polycarbonate volumetric flask and analyzed for mercury with a Leeman Labs inductively coupled plasma emission spectrometer with full account of matrix effects. Mercury levels in the supernatants of absorption experiments were measured by direct introduction and analysis in the plasma spectrometer. The ash content of GHA was determined by combustion of weighed, dry 200.0 mg samples in air at 850 °C for 30 min. The total acidities and carboxylic acid contents of solid humic acids CHA and GHA were determined with literature methods.[23]

Spectrometry. UV−visible and FTIR spectrometry was conducted with previously described instruments and procedures.[2,13]

Adsorption Measurements. Adsorption of uracil on solid GHA was measured with the same 19 solute concentrations as previously employed[13] but with 20.0 mg GHA aliquots and 20.0 mL of each solute solution. Adsorption experiments were conducted at fixed temperatures 5.0, 10.0, 15.0, 20.0, 25.0, 30.0, and 35.0 °C. Experiments with MGHA as the adsorbent were conducted with aqueous solutions of uracil, uridine, and uridine-5′-monophosphate. At each of the above fixed temperatures, 20.0 mg aliquots of MGHA were shaken in glass vials containing 10.0 mL of 0.024, 0.048, 0.072, 0.096, 0.12, 0.18, 0.24, 0.30, 0.36, 0.42, 0.48, 0.54, 0.60, 0.66, 0.72, 0.84, 0.96, 1.08, and 1.20 mM solutions of the respective solutes. The pH of each solution was measured before and after equilibration, which was complete in all cases within 24 h. After centrifugation, the absorbance of each supernatant was measured at the solute absorption maximum. All absorbance readings were reproducible to within ±2%. The equilibrium solute concentration c (M) was calculated with the Beer−Lambert law from the standard calibration plot for each solute. This enabled calculation of the isotherms (amount of solute adsorbed A (mol/g adsorbent) vs c).

Five percent of the 20.0 mg of solid GHA dissolves in the 20.0 mL solutions used with uracil as solute at pH 3.7−4.3. To allow for GHA solubility, a solution with pH 4.0 containing 20.0 mg GHA but no uracil was employed as a blank in UV absorbance measurements of c in the GHA−uracil system from the corrected supernatant uracil spectrum. The resulting isotherm A's were corrected with UV measurements of the blank vs water to allow for 5% GHA solubility. MGHA has negligible solubility up to at least pH 7.0, and no correction for MGHA solubility was necessary to determine the isotherms for solutes uracil, uridine, and uridine-5′-monophosphate adsorption on MGHA.

Data Analysis. The Langmuir model for reversible adsorption at a distinct site, eq 1, predicts eq 2, which can be inverted to give eq 3. If the Langmuir model applies, a plot of $1/A$ vs $1/c$ should be linear with positive slope $1/Kv$ and positive intercept $1/v$. Here, K is the equilibrium constant for reaction 1 and v is the capacity of the site for the solute. Plots of eq 3 for complete isotherms for NAC adsorption on CHA result in linear segments that indicate sequential adsorption steps i = A, B, and C (see, for example, Figure 4 of ref 13). Equation 2 can be rearranged to eq 4. Plots of c/A vs c should have linear segments with positive slopes that also indicate the sequence of adsorption steps (see Results and Discussion section). Plots of eq 3 at different temperatures indicate whether v_i for a particular adsorption step is temperature dependent or not. Plots of $\log K_i$ vs $1/T$, where T is the absolute temperature, give linear plots if one adsorption process occurs in a given step throughout the experimental temperature range. The enthalpy ΔH_i and entropy change ΔS_i for adsorption in each step are calculated

TABLE 1: Analytical Data for Humic Acid Adsorbents

sample	%C[a]	%H[a]	%N[a]	%Ash[b]	Total Acidity[c]	R−COOH[c]	Ar−OH[c,d]
CHA	50.4[e]	5.9[e]	6.4[e]	5.0[e]	4.9	2.0	2.9
GHA[f]	50.5	5.3	1.7	1.5	7.9	3.3	4.6

[a] % w/w expressed on a dry weight, ash-free basis. [b] Determined by combustion at 850°C. [c] Units are mequiv/g HA (average of three determinations). For methods see ref 23. [d] Taken as the difference between columns 6 and 7 (ref 23). [e] Data from ref 13. [f] Hg content of MGHA determined by plasma spectrometry is 9.0% w/w (0.45 mmol/g MGHA) expressed on a dry, ash-free weight basis.

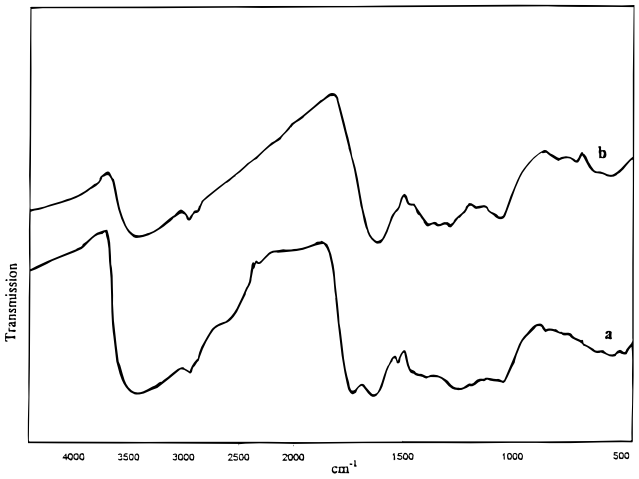

Figure 1. Room-temperature KBr disk FTIR spectra of (a) GHA; (b) MGHA.

from the slope and intercept of eq 5.

$$\mathrm{HA(s) + solute(aq) \rightleftharpoons HA{\cdot}solute(s)}\ (K) \qquad (1)$$

$$A = Kvc/(1 + Kc) \qquad (2)$$

$$1/A = 1/Kvc + 1/v \qquad (3)$$

$$c/A = c/v + 1/Kv \qquad (4)$$

$$\log K_i = -\Delta H_i/2.303RT + \Delta S_i/2.303R \qquad (5)$$

Results and Discussion

We present new data for adsorption of uracil, uridine, and uridine-5′-monophosphate on a humic acid isolated from German peat (GHA) and its tightly bound mercury(II) form (MGHA) over a wide concentration range and at seven temperatures from 5.0 to 35.0 °C. The results are compared with previous data[13] for adsorption of these same solutes on municipal compost-derived humic acid (CHA).

Analytical data for adsorbents CHA and GHA are given in Table 1. The %C and %H and atomic C/H ratios of CHA and GHA are similar and typical of purified HAs.[6−8,10,11,21−23] CHA has the larger %N. GHA is more acidic than CHA, as reflected by its larger carboxylic acid and phenol contents. Table 1 shows that treatment of GHA with mercury(II) acetate and removal of excess reagent and weakly bound mercury(II) by washing the sample several times with water leaves 9.0% w/w (0.45 mmol/g) of bound mercury(II) in dry sample MGHA.

Figure 1 compares the FTIR spectra of GHA and MGHA. The spectrum of GHA is typical of purified HAs.[24−26] Absence of the features for GHA centered at 2500 cm^{-1} (broad, H-bonded COOH) and 1715−1730 cm^{-1} (C═O of −COOH) in the spectrum of MGHA is taken as evidence for mercury(II) binding by carboxylate groups in GHA, as supported by similar X-ray absorption near energy spectra (XANES) and extended X-ray absorption fine structure (EXAFS) data for tightly bound mercury(II) in HAs from different sources and mercury(II) carboxylate standards.[27] HA groups R−COOH/R−COO^- are principal sites for metal and mineral binding.[26,28] Room-temperature demetalation and demineralization of HAs with Chelex and Tiron (4,5-dihydroxy-1,3-benzenedisulfonic acid, disodium salt) greatly increase their solubility, result in the broad feature at 2500 cm^{-1}, and resolves discrete bands in the 1715−1730 cm^{-1} region of their FTIR spectra.[29]

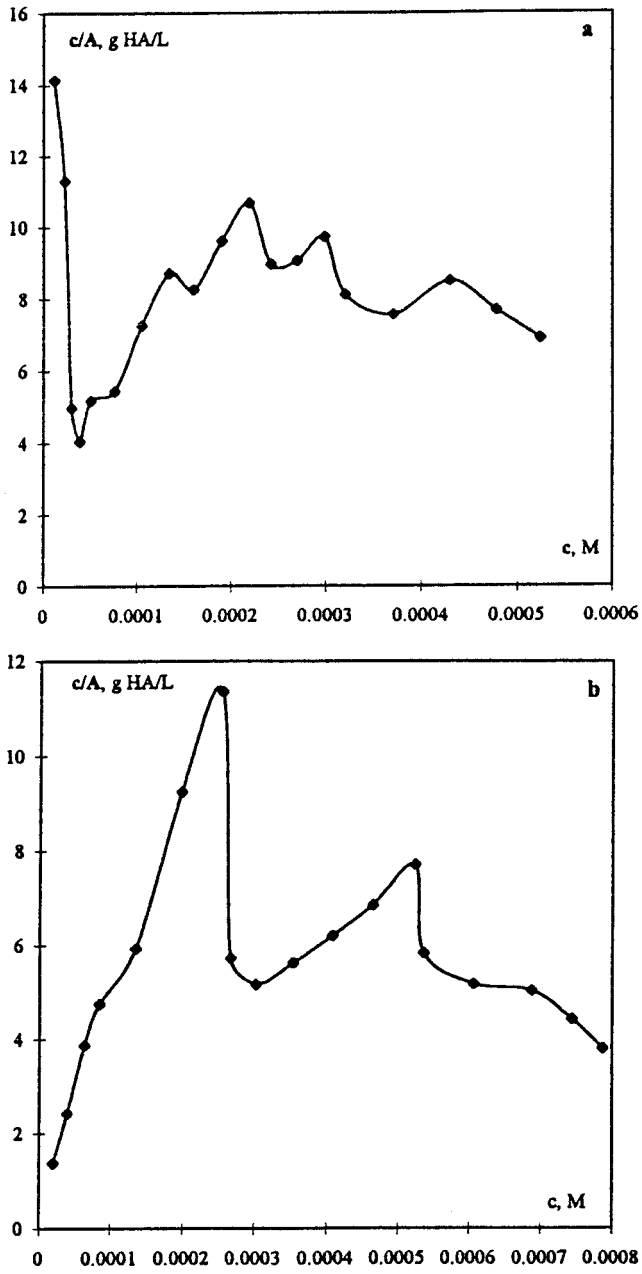

Figure 2. Plots of eq 4 for (a) adsorption of uracil on GHA at 20.0 °C; (b) adsorption of uridine on MGHA at 20.0 °C.

Adsorption Characteristics and Data Analysis. Analyses of isotherms with GHA and MGHA adsorbents indicated that plots of c/A vs c (eq 4) at fixed temperature are helpful in finding (1) the number of detectable Langmuir adsorption steps from linear plot segments with positive slopes $1/v_i$ and (2) the range of c where overlap of one step with another occurs. Success with this approach mainly depends on the c/A and c ranges with positive slopes in plots of eq 4. The plot in Figure 2 a has a negative slope up to $c = 0.040$ mM, and a plot of eq 3 for this data subset has a negative intercept, indicating that v_A increases

TABLE 2: Data for Adsorption on CHa, GHA, and MGHA[a]

		steps								
		CHA			GHA			MGHA		
solute	temp[b]	10^3K_i	υ_i	ΔH_i, ΔS_i	10^3K_i	υ_i	ΔH_i, ΔS_i	10^3K_i	υ_i	ΔH_i, ΔS_i
					Uracil					
A	5.0				34	0.01				
	10.0	1.7[c]	0.02		75	0.01				
	15.0			−30.9, −76	82	0.01	10.0, 44			
	20.0	2700	0.02		see text			irreversible, see text		
	25.0	780	0.01		59	0.03				
	30.0	290	0.01		240	0.04				
	35.0	230	0.01		200	0.08[c]				
		780	⟨υ⟩ 0.01		59	⟨υ⟩ 0.02				
B	5.0				negative υ			34.5	0.05	
	10.0	2.7	0.04		24	0.02[c]		14.8	0.10	
	15.0				1.2[c]	0.07		39.2	0.10	
	20.0	0.6[c]	0.70[c]	2.8, 26	see text		38.9, 140	21.7	0.16	6.6, 29
	25.0	4.1	0.05		6.3	0.06		20.1	0.19	
	30.0	4.2	0.03		41	0.04		31.6	0.22	
	35.0	negative υ			negative υ			39.9	0.24	
	40.0	4.4	0.03							
		4.1	⟨υ⟩ 0.04		6.3	⟨υ⟩ 0.6		20.1	⟨υ⟩ 0.15	
C	5.0				negative υ			1.2	0.23	
	10.0	0.02[c]	3.90[c]		negative υ			0.7	0.52	
	15.0			−9.2, −15	negative υ		61.4	2.2	0.34	8.0, 29
	20.0	0.3	0.90[c]		negative υ		210	3.1	0.36	
	25.0	0.7	0.10		0.8	0.2		2.7	0.43	
	30.0	0.5	0.20		7.1	0.1		3.3	0.46	
	35.0	0.9	0.20		23	0.1		6.2	0.44	
		0.7	⟨υ⟩ 0.17		0.8	⟨υ⟩ 0.13		2.7	⟨υ⟩ 0.40	
					Uridine					
A	5.0							3.2	0.03	
	10.0	10	0.01					3.5	0.04	
	15.0							7.8	0.04	
	20.0	55[c]	0.01	13.1, 65				83.9[c]	0.02	11.1, 42
	25.0	24	0.02					18.4	0.03	
	30.0	6.8[c]	0.01					9.8	0.05	
	35.0	81	0.01					25.5	0.04	
	40.0	83	0.003							
		24	⟨υ⟩ 0.01					18.4	⟨υ⟩ 0.04	
B	5.0							1.8	0.11	
	10.0	negative υ						1.1	0.17	
	15.0							5.2	0.08	
	20.0	1.5	0.05	28.2, 110				6.4	0.09	−6.3, −18
	25.0	2.2	0.09					3.9	0.11	
	30.0	negative υ						3.7	0.11	
	35.0	20	0.02					2.8	0.13	
	40.0	25	0.02							
		2.2	⟨υ⟩ 0.05					3.9	⟨υ⟩ 0.11	
					UMP					
A	5.0							230	0.01	
	10.0	13	0.03					25	0.01	
	15.0							59	0.01	
	20.0	94	0.02	28.3, 120				38	0.01	−22.7, −71
	25.0	360	0.03					12.6	0.02	
	30.0	570	0.01					8.1	0.02	
	35.0	1400	0.01					17	0.02	
	40.0	1300[c]	0.02							
		360	⟨υ⟩ 0.02					11.6	⟨υ⟩ 0.01	
B	5.0							3.2	0.03	
	10.0							6.3	0.03	26.3, 97[d]
	15.0							17	0.02	
	20.0							negative υ		
	25.0							2.0	0.04	−24.7,
	30.0							3.7	0.02	−81[c]
	35.0							see text		
	40.0									
								2.0	⟨υ⟩ 0.03	

[a] All data for adsorption of uracil, uridine, and uridine-5′-monophosphate on CHA in this table are from ref 13. Units: K_i = equilibrium constant for adsorption at HA site I, M^{-1}; υ_i = mmol/g HA; ⟨υ⟩ = average value of υ_i over the experimental temperture range; ΔH_i = kcal mol^{-1}; ΔS_i = cal deg^{-1} mol^{-1}. [b] °C. [c] Excluded from analysis, see refs 13, 14 and text. [d] For data at or above 25.0 °C.

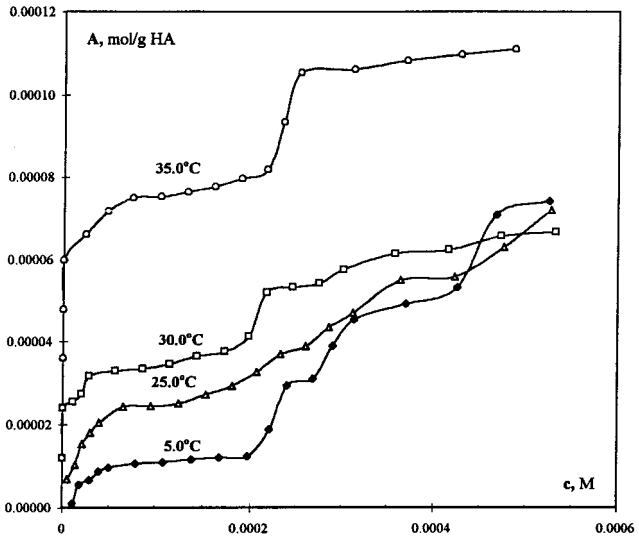

Figure 3. Isotherms for uracil adsorption on GHA.

with increasing c. The range of increasing $c/A = 4-10.4$ g GHA/L with $c = 0.040-0.22$ mM in Figure 2a results from compensating trends $v_A < v_B < v_C$ and $K_A > K_B > K_C$ and the magnitudes of v_i and K_i for uracil adsorption on GHA at 20.0 °C. In Figure 2a, c/A decreases in "waves" with increasing $c > 0.22$ mM. The features at lowest and highest c thus limit the ranges for Langmuir analysis to $c/A = 4-10.4$ g GHA/L and $c = 0.040-0.22$ mM, which are too small to give reliable v_i and K_i parameters for sequential uracil adsorption on GHA at 20.0 °C. In contrast, the ranges $c/A = 1.3-11.4$ g MGHA/L, $c = 0.02-0.24$ mM and $c/A = 5.2-7.7$ g MGHA/L, $c = 0.31-0.52$ mM for which c/A increases with increasing c in Figure 2b allow more confident distinction of sequential adsorption steps. Fortunately, almost all the isotherms with GHA and MGHA adsorbents had the characteristics of Figure 2b. These data were analyzed with eq 3 to give the v_i and K_i parameters in Table 2.

Uracil Adsorption on GHA. Uracil is a neutral molecule[30] in the experimental pH range 3.7−4.3 of this study. Figure 3 shows isotherms for adsorption of uracil on solid GHA at four representative experimental temperatures. At 30.0 and 35.0 °C, GHA strongly adsorbs the lowest concentrations of uracil (as indicated by points on the vertical axis), whereas CHA does not exhibit this phenomenon.[13]

Plots of eq 3 for most of the uracil adsorption data have linear segments for steps A, B, and C that are easier to identify than from inspection of the isotherms (Figure 3). Representative examples are shown in Figure 4. Parameters v_i and K_i calculated at different temperatures from the respective positive slopes and intercepts are collected in Table 2 with previously reported data for adsorbent CHA.[13]

Intercepts in plots of eq 3 for uracil adsorption on GHA in step B at 5.0, 20.0, and 35.0 °C were negative, but v_B at other temperatures are positive and average well (Table 2). Negative intercepts of plots of eq 3 in step C at 20.0 °C and all lower temperatures must have a different origin since the data give positive v_i for other steps at other temperatures (Table 2). An explanation is that v_C for low-temperature uracil adsorption on GHA in step C increases with increasing solute concentration, which results in S-curves (see below).[31]

Site Capacities. Table 2 shows within data precision limits and except as noted above that (1) site capacities v_i for uracil adsorption on CHA[13] and GHA are temperature independent; (2) average site capacity $\langle v_A \rangle$ over the temperature range is somewhat larger with GHA (0.017 mmol/g HA) than with CHA

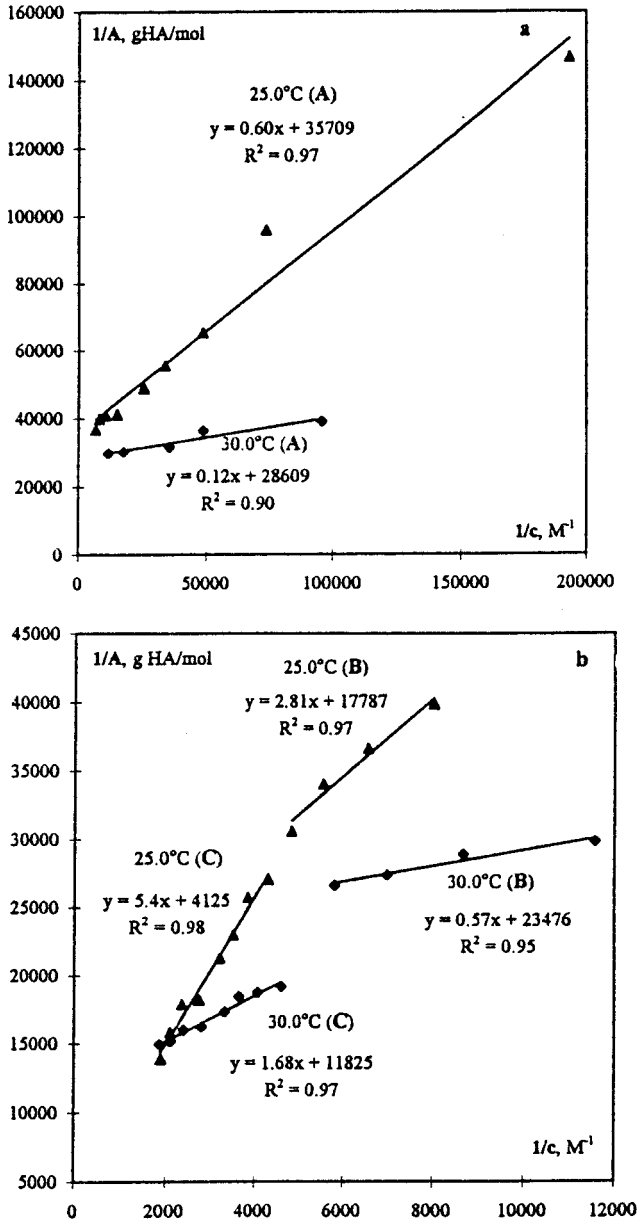

Figure 4. Representative plots of eq 3 for uracil adsorption on GHA at 25.0 and 30.0 °C: (a) step A; (b) steps B and C.

(0.010 mmol/g HA)[13] as adsorbent; (3) $\langle v_B \rangle$ is larger than $\langle v_A \rangle$ and similar for CHA and GHA; and (4) $\langle v_C \rangle$ at 25.0 °C and higher temperatures is the largest $\langle v_i \rangle$ and is larger with CHA as adsorbent than with GHA.

The site capacities follow the general trend $\langle v_C \rangle > \langle v_B \rangle > \langle v_A \rangle$ found previously.[13,14] Similar site capacities $\langle v_A \rangle$ or $\langle v_B \rangle$ or $\langle v_C \rangle$ with CHA and GHA adsorbents show that uracil occupies about the same number of primary adsorption sites in step $i =$ A or B or C and imply that these sites are chemically similar.[15]

Equilibrium Constants. Equilibrium constants K_i for uracil adsorption on GHA follow the general trend found with CHA: $K_C < K_B < K_A$.[13,14] Notable is that K_A for uracil adsorption on CHA at 25.0 °C is about 13 times larger than with adsorbent GHA (Table 2). Otherwise, there is remarkable similarity of K_i at 25.0 °C for uracil adsorption on CHA and GHA. However, this is the result of quite different adsorption enthalpies ΔH_i and entropies ΔS_i (see Table 2 and below). Different interactions with HA adsorption sites are possible with multifunctional molecules such as uracil. Similar site capacities but different thermodynamic parameters in a given step i imply that uracil

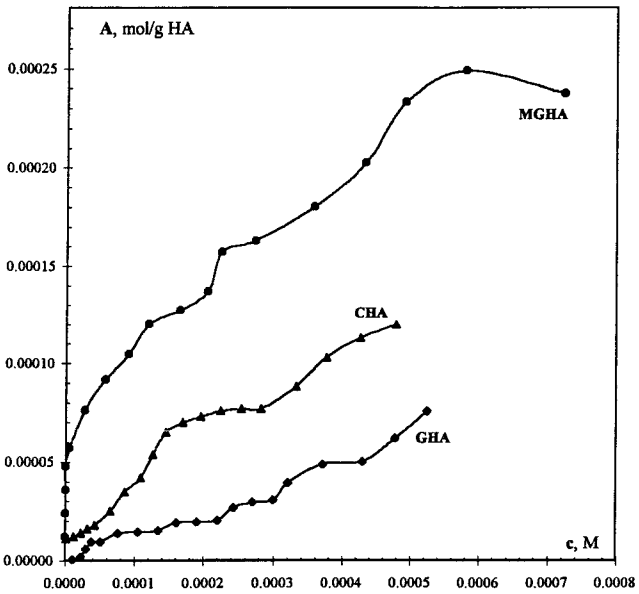

Figure 5. Isotherms for uracil adsorption on CHA (data from ref 13), GHA, and MGHA at 20.0 °C.

also associates with other groups close to the primary adsorption sites and that the primary sites are well separated in CHA and GHA.

Adsorption on MGHA. Analysis of supernatants indicated negligible mercury leaching from MGHA at the highest concentrations of uracil, uridine, and uridine-5′-monophosphate used to measure their adsorption on MGHA. The data thus refer to interactions of these solutes with sites in solid MGHA.

Site Capacities for Adsorption of Uracil on MGHA. The presence of tightly bound mercury in GHA dramatically affects its interaction with uracil (Figure 5). We find the largest $\langle v_i \rangle$ and K_i with MGHA as adsorbent (Table 2). Very strong binding of low concentrations of uracil by MGHA (Figure 5) made it necessary to use higher solute concentrations than employed with CHA[13] and GHA in order to observe subsequent adsorption steps. Unlike the case with mercury-free GHA (Figure 3), strong interaction of low concentrations of uracil with MGHA persists at all temperatures. The amounts of uracil adsorbed in this step labeled A increase from 0.02 mmol/g MGHA at 5.0 °C to 0.085 mmol/g MGHA at 35.0 °C. Also unlike the case with CHA and GHA, site capacities v_B for the first reversible adsorption process labeled B (Figure 6) increase with increasing temperature, while those for step C are temperature independent (Table 2). It appears that site creation[15] by uracil in step B occurs due to the presence of mercury in GHA and is endothermic.

Total average site capacities $\sum\langle v_i \rangle$ are useful for comparison of data for different solutes with a fixed adsorbent.[13−15] If we add $v_A = 0.09$ mmol/g MGHA (at 25.0 °C and representative of very strong uracil binding in step A) to $\langle v_B \rangle = 0.15$ mmol/g MGHA and $\langle v_C \rangle = 0.40$ mmol/g MGHA from Table 2, the result is 0.64 mmol uracil/g MGHA, to be compared with $\sum\langle v_i \rangle =$ 0.21 mmol uracil/g GHA. The difference between these sums, 0.43 mmol uracil/g adsorbent, is the same, within experimental precision, as the mercury(II) content of MGHA (0.45 mmol Hg/g MGHA, Table 1). Thus it appears, *on average*, that each mercury(II) center in MGHA binds one uracil and that mercury binds at GHA sites that do not bind uracil in the absence of mercury(II).

Equilibrium Constants. A lower limit for K_A (M^{-1}) for adsorption of uracil on MGHA can be estimated by assuming that $K_A c \geq 10$ in eq 2 at the lowest solute concentration (0.024 mM) so that A is independent of c, as observed (Figure 5). This gives $K_A \geq 4 \times 10^6$, which is about 1 and 2 orders of magnitude greater than for uracil adsorption on CHA and GHA, respectively, in step A (Table 2). Strongest uracil binding by mercury(II) persists in steps B and C, with the respective K_i being 10 and 4−5 times larger than with no mercury present (Table 2). The K_i for uracil adsorption on MGHA in Table 2 thus refer to uracil binding by mercury(II).

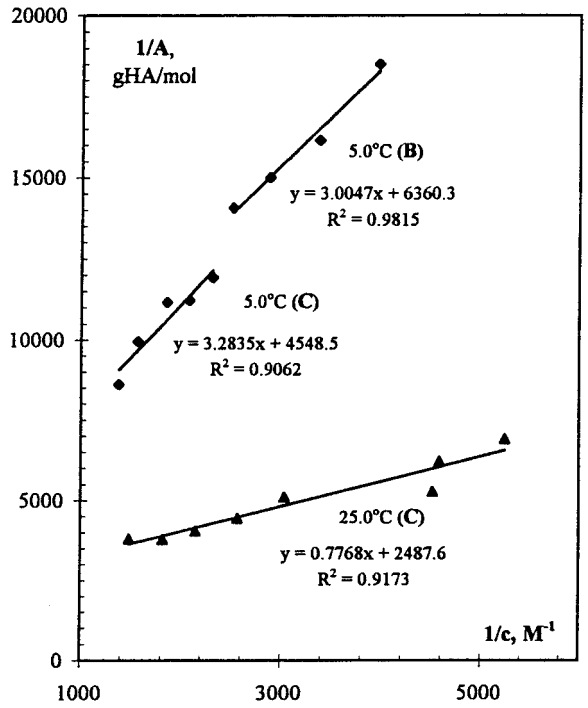

Figure 6. Plots of eq 3 for adsorption of uracil on MGHA at 5.0 and 25.0 °C.

Adsorption of Uridine and Uridine-5′-monophosphate on MGHA. As mentioned, mercury(II) differs from most metals in strongly preferring the soft uracil and thymine nucleobases of the corresponding nucleosides and nucleotides. Strong binding of uracil by mercury in MGHA could occur through its N_1, N_3, or O_4 atoms.[17−20] The N_1 center of uridine and uridine-5′-monophosphate seems unlikely to bind to mercury because it is condensed with the ribose unit. With this assumption, we studied adsorption of uridine and uridine-5′-monophosphate on MGHA for comparison with uracil. Like uracil, uridine is a neutral molecule in the pH range 4.6−5.1 used for the measurements, while uridine-5′-monophosphate is a monoanion[30] in the pH range 3.4−4.6 used to measure its isotherms. These differences check the effects of solute charge and molar mass on the adsorption parameters.[13−15]

Adsorption of uridine and uridine-5′-monophosphate on MGHA exhibits two reversible Langmuir steps labeled A and B. Unlike the case with uracil, no evidence for very strong adsorption of low concentrations of either solute was found (Figure 7), and plots of eq 3 were linear with positive intercepts $1/v_A$ and $1/v_B$ (Figure 8). However, plots of eq 3 for step C have negative intercepts (Figure 8b), indicating that v_C increases with increasing c at the highest uridine and uridine-5′-monophosphate equilibrium concentrations.

Site Capacities. Unlike the case with uracil, adsorption of uridine and uridine-5′-monophosphate on MGHA has v_A and v_B that are independent of temperature. Comparison of $\langle v_A \rangle$ and $\langle v_B \rangle$ parameters in Table 2 indicates the following: (1) $\langle v_A \rangle$ and $\langle v_B \rangle$ are lower than with uracil as solute and compare well with those for uridine and uridine-5′-monophosphate adsorption on CHA.[13] The only exception to this statement is similarity

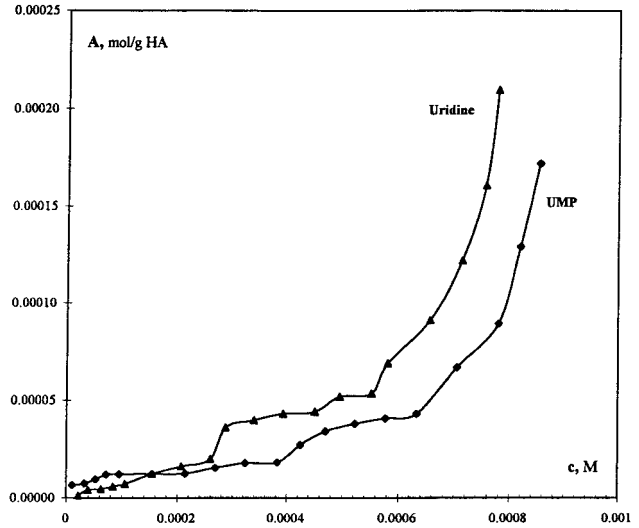

Figure 7. Isotherms for adsorption of uridine and uridine-5′-monophosphate on MGHA at 5.0 °C.

of $\langle \upsilon_B \rangle$ for adsorption of uracil and $\langle \upsilon_B \rangle$ for uridine adsorption on MGHA. With this exception, it appears that uridine and uridine-5′-monophosphate do not bind to mercury(II) in MGHA and that uracil binds to mercury in MGHA through its N_1 atom.

We found[13,14] that temperature independent $\langle \upsilon_i \rangle$ for nucleic acid constituent solutes such as adenine and cytosine are larger than for uracil, and we have interpreted the data with a model in which primary solute adsorption can free up ("create") more of the same adsorption sites, depending on the solute and adsorption step.[15] As noted earlier, plots of eq 3 for adsorption of uracil on GHA in step C at 20.0 °C or lower temperatures have negative intercepts, whereas υ_C are positive and independent of temperature when the adsorbent is MGHA (Table 2). It thus appears that site "creation" in GHA can occur at low temperatures in step C with increasingly high concentrations of uracil, whereas uracil behaves as if site creation does not occur in step C of its interaction with CHA.[13,15]

Equilibrium Constants. As expected from the site capacity evidence, K_A and K_B at 25.0 °C for uridine adsorption on CHA[13] and MGHA are similar (Table 2). Much larger K_A for uridine-5′-monophosphate adsorption on CHA[13] than on MGHA suggests that this solute benefits from interactions with groups near the primary adsorption sites in CHA. Step B was not detected for uridine-5′-monophosphate adsorption on CHA,[13] but υ_B and K_B at 25.0 °C for uridine adsorption on CHA[13] and uridine-5′-monophosphate on MGHA adsorbents are similar (Table 2).

Thermodynamic Parameters. Linear plots of eq 5 indicate a single process for adsorption of a solute by an adsorbent in a given adsorption step. All but one of the K_i data sets in parts 1[13] and 2[14] give linear plots of eq 5 with close to zero, positive, or negative slopes. This indicates that adsorption in one process on CHA can be thermoneutral, exothermic, or endothermic, depending on the solute and adsorption step.

The linear plot in Figure 9a is representative of almost all the available K_i data for adsorption on CHA,[13,14] GHA. and MGHA. This particular plot indicates that adsorption of uridine-5′-monophosphate on MGHA in step A is a single exothermic process (Table 2). By contrast, adsorption of this solute in step B is endothermic at or below 25.0 °C and exothermic at higher temperatures (Figure 9b), as also found for cytidine adsorption on CHA in step C[13] but with smaller differences of ΔH_i and ΔS_i in the low and higher temperature ranges (Table 2). Behavior like that in Figure 9b may be taken as evidence for temperature dependent interactions with groups close to primary

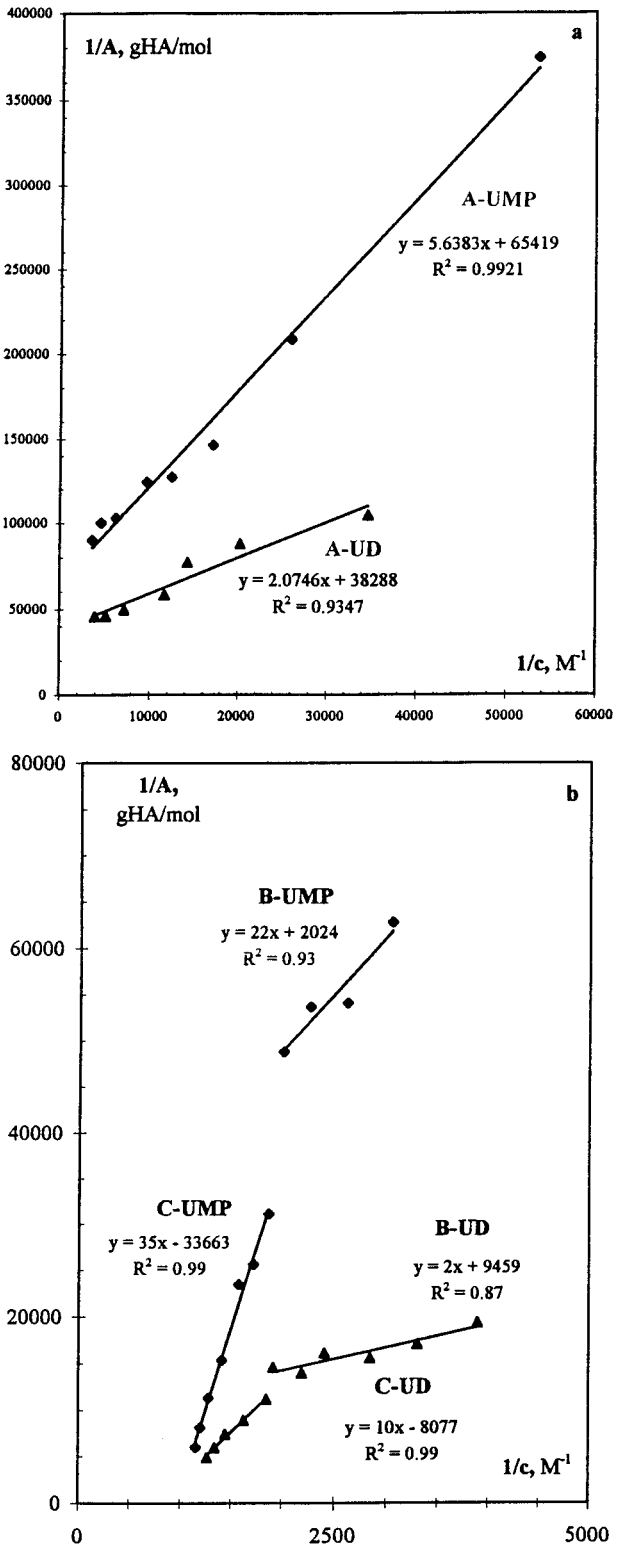

Figure 8. Plots of eq 3 for adsorption of uridine and uridine-5′-monophosphate on MGHA at 25.0 °C.

adsorption sites in HAs, but more examples of such *dual-temperature* adsorption are needed for full understanding.

Correlation of Thermodynamic Parameters. Parts 1[13] and 2[14] demonstrate that a plot of $[\Delta H_i, \Delta S_i]$ data, where ΔH_i and ΔS_i are the enthalpy and entropy change in a given adsorption step with a given solute, are linearly related for all 14 nucleic acid constituents investigated with CHA as the adsorbent. Equation 6 predicts a linear plot if ΔG_i varies much less than

$$\Delta H_i = T\Delta S_i + \Delta G_i \qquad (6)$$

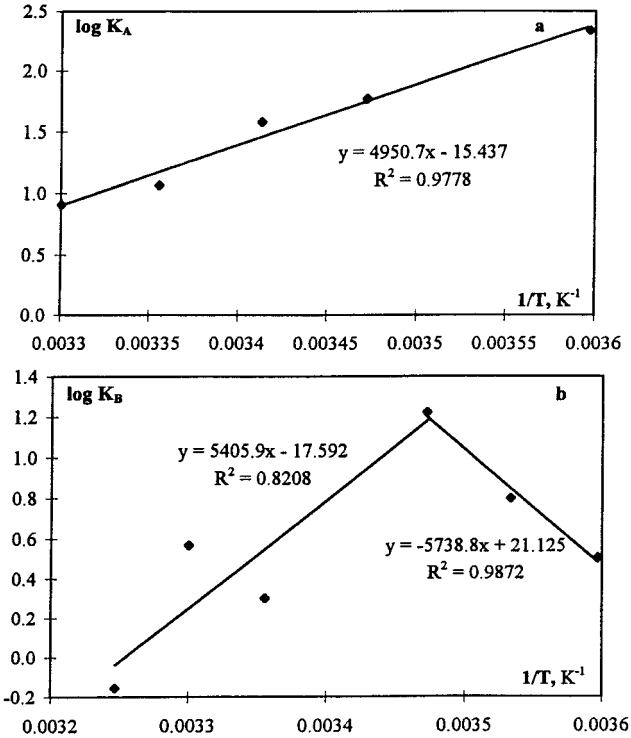

Figure 9. Plots of eq 5 for adsorption of uridine-5′-monophosphate on MGHA in (a) step A; (b) step B.

ΔH_i and ΔS_i for the whole database (as is the case)[13,14] and if all adsorption steps have the same characteristics. A large database (111 data sets) enabled us to test a model[15] for adsorption on CHA consisting of four main steps; (1) primary solute adsorption at, say, a surface A site; (2) freeing up ("creation") of more A sites induced by some solutes as a result of primary adsorption by breaking, say, A···(X,Y) interactions, where X,Y ≠ A; (3) solute adsorption on these newly available A sites; and (4) hydration of X and Y. This model accounts well for adsorption of nucleic acid constituents on the A, B, and C sites of CHA and is consistent with Wershaw's membrane−micelle model for aggregated HAs.[32]

The present study of adsorption on GHA and MGHA was restricted to solutes uracil, uridine, and uridine-5′-monophosphate for reasons stated earlier. Data with more solutes will test the model[15] with metal-loaded and unloaded HAs from different sources. In the meantime we can report a linear correlation of the present data based on eq 6.

Figure 10 shows two plots of eq 6. The lower line refers to sequential, reversible adsorption of solutes uracil, uridine, and uridine-5′-monophosphate on CHA.[13] Its slope is 307 K (34 °C), and its intercept is −6.0 kcal mol^{-1}. The upper line correlates data for sequential, reversible adsorption of the same solutes on GHA and MGHA. Its slope is 299 K (26 °C), and its intercept is −1.4 kcal mol^{-1}. Thus, on average, adsorption of uracil, uridine, and uridine-5′-monophosphate on GHA and MGHA is 4.6 kcal mol^{-1} more endothermic than on CHA.[13] Inclusion of the whole database[13,14] for sequential, reversible adsorption of 14 nucleic acid constituents on CHA in all detected steps covers the ranges $\Delta H_i = -55$ to 65 kcal mol^{-1} and $\Delta S_i = -167$ to 240 cal deg^{-1} mol^{-1} and gives a linear plot with slope 297 K (24 °C) and intercept −5.2 kcal mol^{-1} .[15]

The significance of the different slopes and intercepts in Figure 10 will be clearer when data for adsorption of more NAC

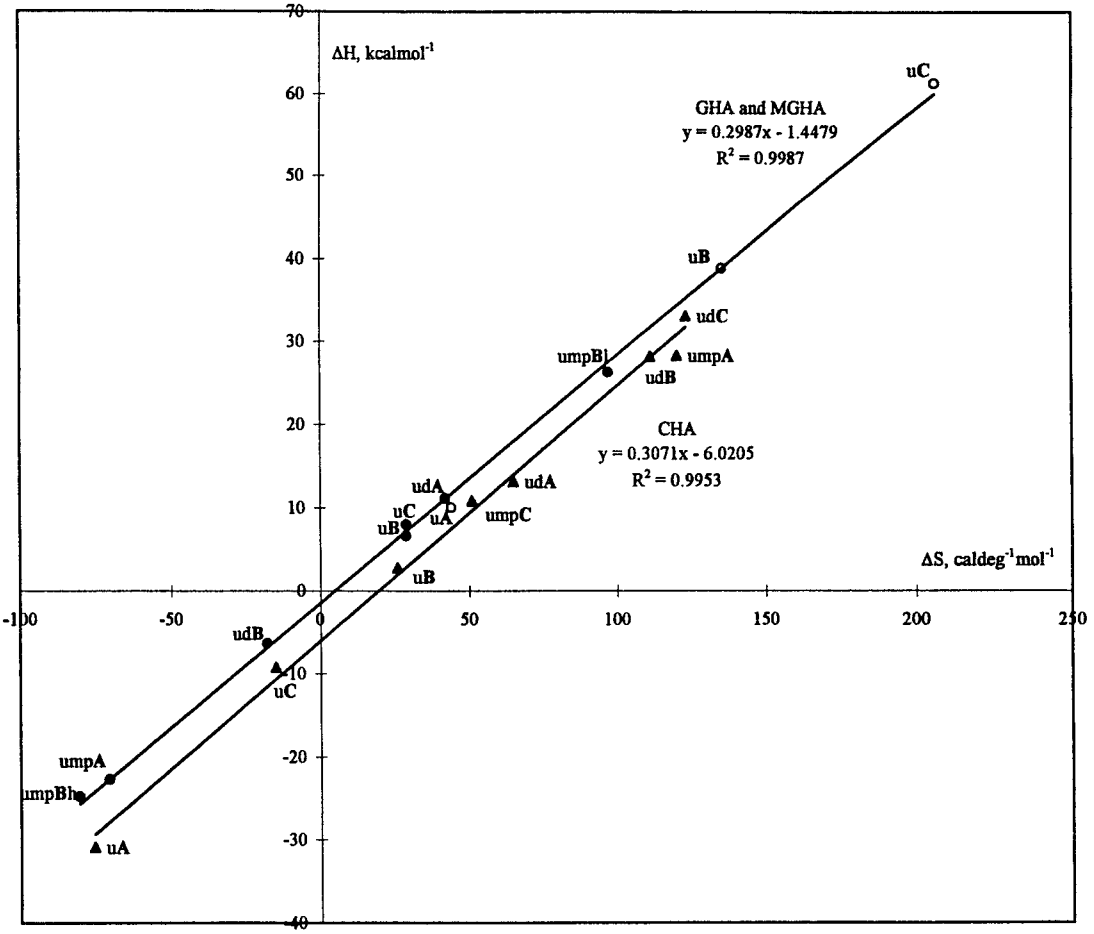

Figure 10. Plots of ΔH_i vs ΔS_i, where ΔH_i and ΔS_i are the enthalpy and entropy changes of a given solute in a given adsorption step A, B, or C, for adsorption of uracil (u), uridine (ud), and uridine-5′-monophosphate (ump) on CHA (▲); GHA (○); and MGHA (●).

solutes on GHA, MGHA, and other HAs are available to test the model proposed for CHA.[15] In the meantime we note the following main features of Figure 10.

(1) The data for adsorption of uracil, uridine, and uridine-5′-monophosphate on GHA and MGHA fit within experimental precision on a single line that is distinct from the correlation with CHA as adsorbent.

(2) Adsorption of uracil on CHA is thermoneutral or exothermic, depending on the adsorption step (Table 2). Figure 10 shows that adsorption of uracil on GHA is 30−70 kcal mol^{-1} more endothermic than on CHA, depending on the adsorption step, and that ΔS_i are correspondingly more positive.

(3) The presence of mercury(II) in GHA reduces the ΔH_i and ΔS_i ranges so that they encompass those with adsorbent CHA and become more exothermic. We concluded earlier that the parameters for MGHA refer to adsorption on mercury(II), and for this reason the lines for CHA and MGHA should not coincide.

Freeze-dried GHA has a fibrous, fractal morphology, while CHA and MGHA have the "chunky" morphology typical of vacuum oven dried HAs.[7,33] As noted, GHA is more soluble at pH 4 than CHA or MGHA. This evidence and the differences noted in Figure 10 suggest that oven-dried and mercury-loaded, freeze dried HAs have "tighter" intra- and intermolecular (A,B,C)···(X,Y) interactions that affect their adsorption of uracil, uridine, and uridine-5′-monophosphate. Whether this is the case with other HAs, metals present, and solutes is the subject of ongoing investigations. The results will be helpful in understanding sorptive properties of humic substances in soils, plants, and sediments.[12−15]

Acknowledgment. We are grateful to Staatsbad Pyrmont AG for the peat source. E.A.G. thanks the Ministry of Agriculture of Egypt for study leave to participate in this work. N.K.G., M.E.G., and N.A.S. gratefully acknowledge Northeastern University for undergraduate research support. We thank undergraduate students Aleksandr Cherkasskiy, Kelly O'Donaughy, Tammy Smith, and Marcy Vozzella for technical assistance and a reviewer for perceptive comments. This is contribution Number 706 from the Barnett Institute at Northeastern University.

References and Notes

(1) Khairy, A. H.; El-Gendi, S. S.; Bhagdadi, H. H. *De Natura Rerum*. **1991**, *5*, 76.

(2) Ghabbour, E. A.; Khairy, A. H.; Cheney, D. P.; Gross, V.; Davies, G.; Gilbert, T. R.; Zhang, X. *J. Appl. Phycol*. **1994**, *6*, 459. Radwan, A.; Willey, R. J.; Davies, G.; Fataftah, A.; Ghabbour, E. A.; Jansen, S. A. *J. Appl. Phycol*. **1997**, *8*, 545. Radwan, A.; Davies, G.; Fataftah, A.; Ghabbour, E. A.; Jansen, S. A.; Willey, R. J. *J. Appl. Phycol*. **1997**, *8*, 553.

(3) Alberts. J. J.; Filip, Z. In *Humic substances in the global environment: Implications for human health*; Senesi, N., Miano, T. M., Eds.; Elsevier: Amsterdam, 1994; pp 781−790, and references therein.

(4) *Humic substances in soil and crop sciences: Selected readings.* MacCarthy, P., Clapp, C. E., Malcolm, R. L., Bloom, R. R., Eds.; American Society of Agronomy: Madison, WI, 1990.

(5) Rashid, M. A.; King, L. H. *Geochim. Cosmochim. Acta* **1970**, *34*, 193. Gillam, A. H.; Riley, J. P. *Anal. Chim. Acta* **1982**, *141*, 287.

(6) Aiken, G. R.; McKnight, D. M.; Wershaw, R. L.; MacCarthy, P. In *Humic substances in soil, sediment and water*; Aiken, G. R., McKnight, D. M., Wershaw, R. L., MacCarthy, P., Eds.; Wiley-Interscience: New York, 1985.

(7) Ziechmann, W. *Humic substances*; BI Wissenschaftsverlag, Mannheim, 1993.

(8) *Humic substances II: In search of structure.* Hayes, M. H. B., MacCarthy, P., Malcolm, R. L., Swift, R. S., Eds.; Wiley-Interscience: New York, 1989.

(9) Schulten, H.-R.; Schnitzer, M. *Naturwiss*. **1995**, *82*, 487, and references therein.

(10) Pierce, R. H., Jr.; Felbeck, G. T., Jr. *Proc. Int. Meet. Humic Subst.*, Nieuwersluis 1972, p 217. We have found that use of 2:1v/v benzene/methanol as a pre-extractant gives products closely similar to HAs obtained from the same source with the more elaborate pre-extraction protocol recommended by Scheffer et al.[11]

(11) Scheffer, F.; Ziechmann, W.; Pawelke, G., *Z. Pflanzenernahr. Bodenk*. **1960**, *90*, 58.

(12) Vieth, W. R. *Diffusion in and through polymers*; Oxford University Press: New York, 1991. Xing, B.; Pignatello J. J.; Gigliotti, B. *Environ. Sci. Technol*. **1996**, *30*, 2432, and references therein. Xing, B.; Pignatello J. J. *Environ. Sci. Technol*. **1997**, *31*, 797. Xing, B.; Pignatello, J. J. *Environ. Toxicol. Chem*. **1996**, *15*, 1282. Chiou, C. T.; Lee, J. F.; Boyd, S. A. *Environ. Sci. Technol*. **1990**, *24*, 1164. Chiou, C. T.; Rutherford, D. W.; Manes, M. *Environ. Sci. Technol*. **1993**, *27*, 1587.

(13) Khairy, A. H.; Davies, G.; Ibrahim, H. Z.; Ghabbour, E. A. *J. Phys. Chem*. **1996**, *100*, 2410.

(14) Khairy, A. H.; Davies, G.; Ibrahim, H. Z.; Ghabbour, E. A. *J. Phys. Chem*. **1996**, *100*, 2417.

(15) Davies, G.; Ghabbour, E. A.; Khairy, A. H.; Ibrahim, H. Z. *J. Phys. Chem*. **1997**, *101*, 3228.

(16) *The chemistry of mercury*; McAuliffe, C. A., Ed.; Macmillan: London, 1977.

(17) Simpson, R. B. *J. Am. Chem. Soc.* **1964**, *86*, 2059. Kuklenyik, Z.; Marzilli, L. G. *Inorg. Chem.* **1996**, *35*, 5654.

(18) Carrabine, J. A.; Sundaralingam, M. *Biochemistry*, 1971, *10*, 292.

(19) Hodgson, D. J. *Progr. Inorg. Chem.* **1977**, *23*, 211, and references therein.

(20) Mansy, S.; Chu, G. Y. H.; Duncan, R. E.; Tobias, R. S. *J. Am. Chem. Soc*. **1978**, *100*, 607, and references therein.

(21) Stevenson, F. J. In *Methods of soil analysis. Part 2: Chemical and microbiological properties*; Black, C. A., Evans, D. D., White, J. L., Ensminger, L. E., Clark, F. E., Eds.; American Society of Agronomy: Madison, WI, 1965; p 1414.

(22) Schnitzer, M.; Khan, S. U. *Humic substances in the environment*; Dekker: New York, 1972; pp 288−292.

(23) Schnitzer, M. *Proc. Int. Meet. Humic Subst*., Wageningen, 1972, pp 293−310. Schnitzer, M.; Gupta, U. C. *Soil Sci. Soc. Am. Proc.* **1964**, *29*, 274.

(24) Chen, Y.; Senesi, N.; Schnitzer, M. *Geoderma* **1978**, *20*, 87.

(25) Johnston, C. T.; Davis, W. M.; Erickson, C.; Delfino J. J.; Cooper W. T. In *Humic substances in the global environment: Implications for human health*; Senesi, N., Miano, T. M., Eds.; Elsevier: Amsterdam, 1994; pp 145−152, and references therein.

(26) Senesi, N. *Trans. 15th World Congr. Soil Sci*. **1994**, *3A*, 384.

(27) Buermann, W.; Budnick, J.; Davies, G.; Fataftah, A.; Ghabbour, E. A. Unpublished results.

(28) Wershaw, R. L.; Llaguno, E. C.; Leenheer, J. A. *Colloids Surf.* **1996**, *108*, 213, and references therein.

(29) Jansen, S. A.; Paciolla, M.; Ghabbour, E. A.; Davies, G.; Varnum, J. M. *Mater. Sci. Eng*. **1996**, *C4*, 182. Davies, G.; Fataftah, A; Cherkasskiy, A.; Radwan, A.; Jansen, S. A.; Paciolla, M.; Ghabbour, E. A. *Proc. 8th Int. Meet. Humic Subst.*, Wroclaw, Poland, 1997.

(30) Barton, J.; Lippard, S. J. In *Nucleic acid-metal ion interactions*; Spiro, T. G., Ed.; Wiley: New York, 1980; pp 33−107.

(31) Giles, C. H.; MacEwan, T. H.; Nakhwa, S. N.; Smith, D. *J. Chem. Soc*. **1960**, 3973.

(32) Wershaw, R. L. *J. Contamin. Hydrol*. **1986**, *1*, 29. Wershaw, R. L. *Environ. Sci. Technol*. **1993**, *27*, 814. Wershaw, R. L. Membrane-micelle model for humus in soils and sediments and its relation to humification. US Geological Survey Water-Supply Paper 2410, 1994.

(33) Radwan, A.; Willey, R. J.; Davies, G. *J. Appl. Phycol.* **1997**, *9*.